NANO LETTERS

2006
Vol. 6, No. 12
2881−2886

High Throughput Quantification of Protein Expression of Cancer Antigens in Tissue Microarray Using Quantum Dot Nanocrystals

Arezou A. Ghazani,[†,‡,§] Jeongjin A. Lee,[‡,§] Jesse Klostranec,[‡,§] Qing Xiang,[‡,§] Ralph S. Dacosta,[||] Brian C. Wilson,[||] Ming S. Tsao,[†,⊥] and Warren C. W. Chan*[,‡,§,#,+]

Division of Applied Molecular Oncology, Ontario Cancer Institute, Toronto, Ontario M5G 2M9, Canada, The Terrence Donnelly Centre for Cellular and Biomolecular Research, Toronto, Ontario M5S 3E1, Canada, Institute of Biomaterials and Biomedical Engineering, University of Toronto, Ontario M5S 3G9, Canada, Department of Medical Biophysics, University of Toronto, Toronto, Ontario M5G 2M9, Canada, Department of Pathology, Princess Margaret Hospital, University Health Network, Toronto, Ontario M5G 2M9, Canada, Department of Materials Science & Engineering, University of Toronto, Toronto, Ontario M5S 3E4, Canada, and Department of Chemistry, University of Toronto, Toronto, Ontario M5S 3H6, Canada

Received September 7, 2006; Revised Manuscript Received October 28, 2006

ABSTRACT

We developed and validated a novel method for quantifying protein expression of cancer tumors in an accurate, sensitive, and high throughput format. This technique integrates quantum dots, tissue microarray, optical spectroscopy, and algorithm design for analysis of tumor biopsies. The integration of this method for tissue analysis in the clinic bears potential impact for improving the diagnosis and treatment of cancer.

Tissue microarray (TMA) is an invaluable tool for simultaneous histological analysis of hundreds of archival tumor biopsies.[1,2] Current research on biomarkers of tumor progression includes microscopic examination of hundreds of tissue samples and evaluation of protein expression levels. The intensity of cancer markers, as determined by visual analysis of colorimetric stains, is used to define a numerical score for staging of tumor biopsies[3] and can be subjected to inter- and intraobserver variability.[4] Quantification of pathology markers has been attempted using standard immunohistochemistry.[5] The numerical categories created by this method however, provide merely semiquantitative values[6,7] and a limited range especially at a very low or high expression level. Several automated methods have also been used to determine localization and quantification of target antigens.[8−10] The precept of these techniques is protein expression analysis through acquisition of fluorescence images obtained from conventional fluorescence dyes. The intensity and accuracy of this quantification method can be compromised by the photobleaching property of fluorophores.[11] Furthermore, the sensitivity of quantitative analysis of protein expression can be affected by tissue autofluorescence. In archival tumor samples, tissue autofluorescence is due to light absorption and scattering from endogenous proteins such as elastin, fibronectin, and collagen,[12,13] from nucleic acids,[14] and from tissue preparation processing and fixation.[13] Given the excessive photobleaching and low signal-to-noise ratios of fluorescent dyes,[15] they are indeed poor candidates for antigen quantification studies. Thus, the feasibility of a sensitive expression profiling and in situ quantification of cancer markers in formalin fixed paraffin embedded (FFPE) biopsies, the most valuable archival tumor specimen, is restricted by the properties of fluorescent molecules and techniques currently used in the laboratory and diagnostic settings.

With the advent of nanotechnology, quantum dot (QD) nanocrystals hold a novel and promising approach for the quantification of antigen-derived markers in FFPE tissue samples. The large Stokes shift (i.e., the difference between

* Corresponding author. warren.chan@utoronto.ca
[†] Division of Applied Molecular Oncology, Ontario Cancer Institute.
[‡] The Terrence Donnelly Centre for Cellular and Biomolecular Research.
[§] Institute of Biomaterials and Biomedical Engineering, University of Toronto.
[||] Department of Medical Biophysics, University of Toronto.
[⊥] Department of Pathology, Princess Margaret Hospital.
[#] Department of Materials Science & Engineering, University of Toronto.
[+] Department of Chemistry, University of Toronto.

10.1021/nl062111n CCC: $33.50
Published on Web 11/17/2006

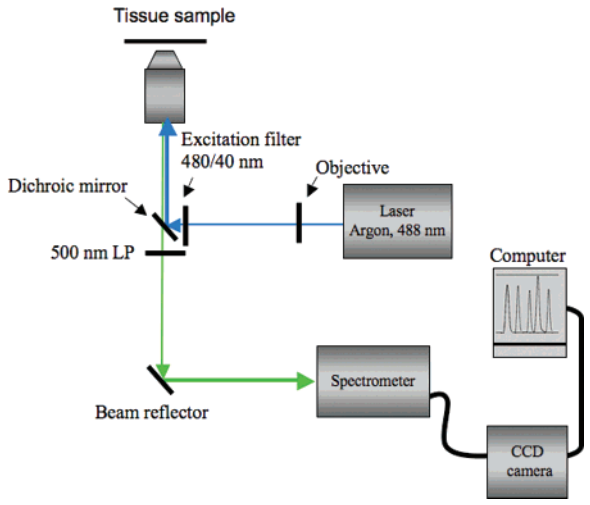

Figure 1. Diagram of the optical spectroscopy system. Wavelength-resolved fluorescence spectroscopy was accomplished by integrating an inverted Olympus microscope with a laser excitation source, a spectrometer, and a CCD camera. The tissue sample is excited using an argon laser at 488 nm. The emission from the tissue sample is collected by a 20× objective (0.75 NA) and passed through a dichroic mirror and a 500 nm long pass (LP) filter. The signal is then dispersed into a spectrum through the spectrometer and detected by a CCD camera. A spectrum indicating the fluorescence emission is depicted.

the excitation and emission wavelengths)[16,17] and high molar extinction coefficients of QDs[16] allow for obtaining high signal sensitivity and thereby minimizing the autofluorescence effect in biological imaging applications. In comparison to organic dyes, QDs have a molar extinction coefficient on the order of $(0.5-5) \times 10^6\ M^{-1}\ cm^{-1}$, about 10−50 times larger than that of organic dyes.[16,18] Consequently, QDs absorb more photons at the same excitation photon flux, leading to significantly brighter signals compared to traditional organic dyes.[19] Furthermore, QD fluorescence is less prone to photobleaching as compared to traditional fluorophores.[20] This could lead to a more sensitive and accurate signal detection. The attractive properties of QDs have subjected them to many cancer-related studies including recently in imaging tumor vasculature,[21] study of apoptosis,[22] and gene expression analysis.[23,24]

In this study, we introduce a novel approach for profiling of protein expression of tumors in a quantitative manner. We employ QD bioconjugates in conjunction with an optical spectroscopy system with potential to detect single molecule fluorescence, the ultimate in detection sensitivity, for high throughput analysis of target antigens on tissue microarrays. With this optical spectroscopy configuration, measurment of the fluorescence emission of a single QD in a localized area has been demonstrated.[20] A schematic of the optical spectroscopy system is shown in Figure 1. To circumvent the limitations associated with tissue autofluorescence, we have also developed a background subtracting algorithm that automatically removes tissue autofluorescence signal, as determined by the optical spectroscope using tissue slides with no tumor specific staining, from total signal (i.e., tumor derived and autofluorescence signals) to produce tumor antigen derived values. We have also developed algorithms that quantitatively analyze tissue cores for tumor antigen derived signals by normalizing the values to the cellular content and finally plot a multiplexed graph (i.e., combined analysis of several antigens at once) of cancer biomarkers on a tissue microarray slide. Overall, the use of these technologies allows for the analysis of high-density tissue microarray data in an automated, accurate, sensitive, and efficient manner.

QD-based immunostaining of membrane epidermal growth factor receptor (EGFR), pan cytokeratin, and E-cadherin in lung cancer xenografts was performed on FFPE tissue microarray slides (see Supporting Information for detailed experimental procedure). Lung cancer xenografts were established by implanting lung carcinoma cell lines MGH7, RVH-6849, A549, H460, H1264, MGH8, H520, and H157 into ventrolateral flanks of Severe Combined Immune Deficiency (SCID) mice (as outlined in the Supporting Information). Tumors of size 1−2 cm were surgically resected after 4 weeks, fixed in formalin, and embedded in paraffin according to the standard histological procedures for preservation of human tissue biopsies. The TMA cohort was constructed from the xenograft tumors using a tissue arrayer. Tissue cores measuring at 0.6 mm in diameter were spaced 0.8 mm apart on a recipient block. Tissue sections were subsequently cut at 5 μm thick sections and placed on a glass microscope slide. Deparaffinization and heat-induced proteolytic epitope retrieval were performed as outlined in the Supporting Information. The pattern of antibody expression was compared to that obtained from an organic dye, Alexa 488 (Supporting Information). There was undetectable nonspecific binding observed for QD staining of tissues using this strategy. The nonspecific binding could vary depending on QD surface coating, tissue types, and tissue sample preparation.

Optical spectroscopy (with a fluorescence emission resolution of <1 nm) was accomplished by integrating an inverted Olympus microscope, a spectrometer, and a charge-coupled device (CCD) camera (Figure 1). The excitation source was provided by an argon−krypton laser with 488 nm emission. A dichroic filter was used to reflect the laser light and to pass the Stokes-shifted fluorescence signals. The signal was collected for each microarray core. We made modifications to the system to allow reading of the entire TMA core of 0.6 mm in diameter by placing a 5× objective lens between the laser and the microscope to expand the laser beam. Sensitivity can be somewhat compromised by this strategy, as the output of fluorescent signal is directly related to power density. However, the increased spot size allowed fluorescence signal from the entire microarray core to be analyzed to avoid any experimental bias due to intratumoral heterogeneity in tissue specimen. This in turn leads to an improved accurate quantification of antigen-derived signals. To demonstrate the feasibility of quantifying cancer antigens in tissue samples, lung carcinoma tissue microarray slides were stained separately for cytokeratin, EGFR, and E-cadherin using QDs. Fluorescence images of the tissue stains from an A549 core on the array are depicted in Figure 2A, while a corresponding

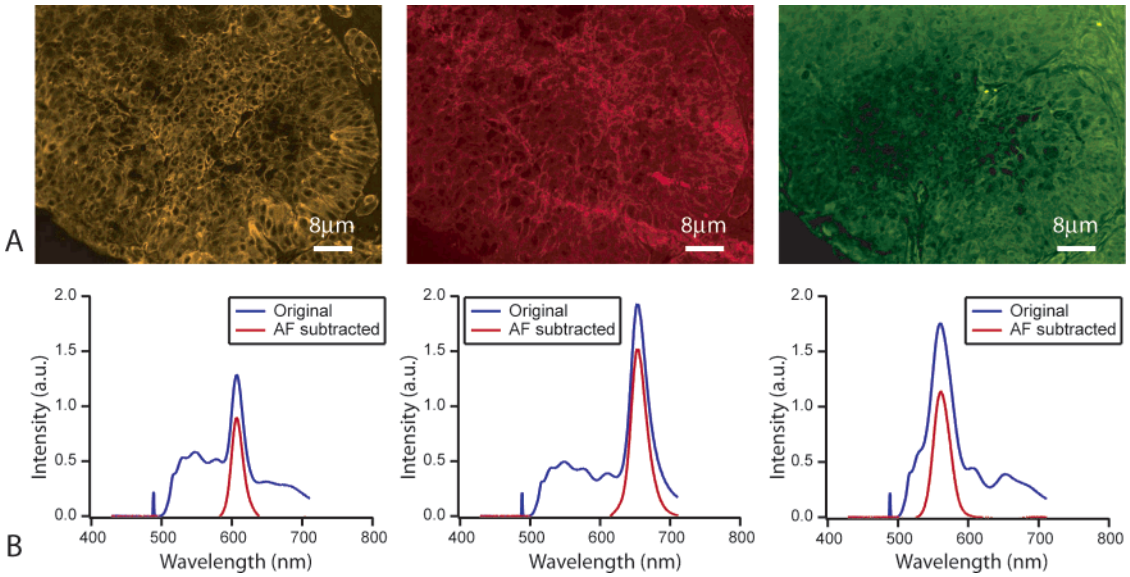

Figure 2. QD-based immunostaining and quantification of tumor antigens. (A) FFPE A549 xenograft sections were labeled for E-cadherin (left), EGFR (middle), and cytokeratin (right). Images were obtained using a 20× (0.75 NA) objective lens. (Filters: excitation = 488 nm; emission = 565/40 nm, 605/40 nm, and 655/40 nm for QDs emitting at 565, 605, and 655 nm, respectively.) (B) The protein expression profile of the antigens as detected by optical spectroscopy is shown in the corresponding figures. The autofluorescent signal is removed from the antigen derived signal using the *D-Noise* algorithm. The mean intensity values of the signals were subsequently calculated using the *Normalizer* algorithm. AF refers to autofluorescence.

spectrum obtained using the optical spectroscopy technique of the entire tissue is shown in Figure 2B.

For accurate determination of antigen-derived signals, background autofluorescence was removed and excluded from the analysis. Tissue autofluorescence is due to light absorption of endogenous protein and cellular content such as collagen,[12,14] co-enzymes, and amino acids.[14,25] Different tissue sections on a microarray contain varying levels of endogenous proteins and thus different levels of autofluorescent signal (Supporting Information). The background autofluorescent signal, therefore, was obtained in each core as determined by a tissue microarray slide with no tumor-specific staining. Any background signal was automatically removed by subtracting tissue autofluorescence from the total signal (autofluorescent and antigen derived signals) using the *D-Noise* algorithm (Figure 2B). This task is feasible with QDs due to their high level of signal intensity well detectable over tissue autofluorescent background.

Accurate tumor antigen quantification is also contingent upon isolation and selection of the signals only from the expression of tumor antigens and not from normal stroma and benign epithelial cells. A method referred to as masking, commonly used in tissue pathology using immunohistochemistry (enzyme based) methods,[26] is generally performed to locate epithelial cells and use them as a tool to standardize tumor measurements to cellular content. This is important, as tissue sections may well differ in cellular density (i.e., cell count and arrangement per area). In our study, a mask was derived from QD immunolabeling of the lung carcinoma tumor sections using pan-cytokeratin staining, a marker for epithelium cells. By use of our *Normalizer* algorithm, the mean signal intensity value from antigen-derived staining was obtained and divided by the cytokeratin signal, thereby normalizing each core to cellular content. Subsequently, the *Multiplexer* algorithm combined the normalized values of all antigens expression in each core to create a composite graph of expression profile across the entire array (Figure 3). A TMA slide and a composite fluorescent image obtained from individual QD immunostaining (i.e., each TMA was stained separately and the images compiled together to render a multi-color image) of an A549 TMA core against EGFR, E-cadherin, and cytokeratin is depicted in parts A and B of Figure 3 while a corresponding analysis of data is shown in Figure 3C.

In order to examine the accuracy and fidelity of this protein quantification system, QD-based immunoassays were conducted on the microarray and analyzed for FFPE lung carcinoma xenografts of MGH7, RVH-6849, A549, H460, H1264, MGH8, H520, and H157, known to have a differential level of expression for membrane EGFR. EGFR was chosen advisedly for the validation study, as the antibody is well characterized for FFPE tissue specimen in the laboratory. Moreover, the mRNA transcript encoding for EGFR has a long half-life and is therefore stable for quantitative analysis as compared to other markers. Optical spectroscopy was performed and quantitative analysis of fluorescent signals from EGFR was obtained in a single staining experiment. The fluorescence signal from the xenografts was measured and analyzed using our algorithm as described above. Subsequently, the endogenous RNA level of EGFR was measured using quantitative real time polymerase chain reaction (Q-RT-PCR) (see Supporting Information for detailed experimental procedure). The quantitative values of EGFR in xenograft tissues were compared using both methods and showed a strong statistical correlation of 0.90 (Figure 4).

Broad absorption spectra of QDs make them amenable to excitation with single light source. We examined whether

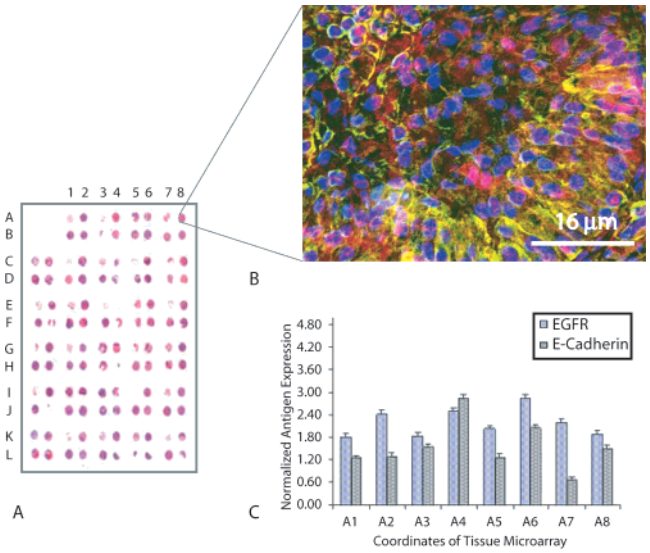

Figure 3. Quantification analysis of cancer-derived antigens in tissue microarray. Tissue cores on a tissue microarray (hematoxylin and eosin image, A) were stained for EGFR, cytokeratin, and E-cadherin. The fluorescent image is a composite picture of the antigens detected by individual QD immunostaining (of different color emission) for each of the targets. 4′,6-Diamidino-2-phenylindole (DAPI) staining is used to locate nuclei in blue (B). Images were taken at 40× (0.85 NA). (Filters: excitation = 360/40 nm; emission = 565/40 nm, 605/40 nm, and 655/40 nm for QDs emitting at 565, 605, and 655 nm and 460/50 nm for DAPI, respectively). The *Normalizer* algorithm normalizes tumor expression values (EGFR and E-cadherin) for epithelial content (cytokeratin). The *Multiplexer* algorithm creates a composite profile of tumor antigen values in each core (C). Cores A1 to A8 correspond to lung cancer xenografts RVH-6849, MGH8, MGH7, H520, H460, H157, H1264, and A549, respectively.

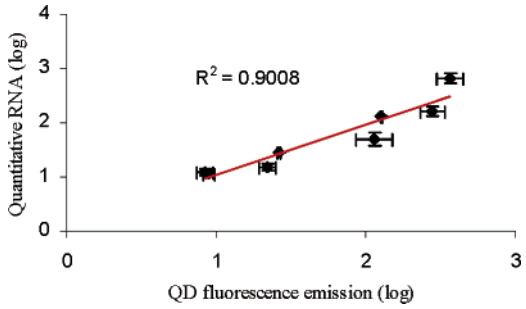

Figure 4. Comparison of data obtained from quantification of protein expression using QD-based immunolabeling and Q-RT-PCR ($n = 8$). The differential expression level of protein was measured by optical spectroscopy after immunolabeling of EGFR with QD bioconjugates on lung carcinoma xenografts of MGH7, RVH-6849, A549, H460, H1264, MGH8, H520, and H157. The endogenous level of RNA transcript for EGFR was measured in the FFPE tissue sections using Q-RT-PCR. The correlation coefficient was found to be 0.90.

concurrent detection of antigens using QD-based multiplex staining on the same tissue can be used for quantitative analysis of protein expression. The level of antigen expression from EGFR, E-cadherin, and cytokeratin in a multiplexed simultaneous staining using 655, 605, and 565 nm QDs, respectively, was compared to those obtained from separate staining experiments for each antigen. The same QDs were used for both the multiplex and single staining experiments to keep the comparative studies consistent. The emission spectra obtained from the multiplexed experiment showed a strong enhancement of the 655 nm signal and reduction of the 605 and 565 nm signals (Figure 5). The values produced by multiplexed staining differ from expected antigen levels obtained from individual staining. The results suggest that fluorescence resonance energy transfer (FRET) may cause the inaccurate measurements in multimarker analysis of the same tissue. FRET is a dipole−dipole interaction process between excited electrons of two molecules, whereby energy from an excited fluorophore (donor) is transferred to an acceptor fluorophore without emission of a photon.[27] In organic fluorescent dyes and QDs alike, FRET is contingent upon the overlap of the donor emission spectrum and the acceptor absorption spectrum.[28] This in turn results in the enhancement of acceptor fluorescence and quenching of donor fluorescence. The efficiency of FRET depends on the spatial distance between molecules as well as fluorescent (hence antigen) concentration.[29] The former, in quantitative measurements of tumor antigen, is unknown, and the latter is sought to be measured. Therefore, in such a case where two unknowns are present and the conditions of the expression level may not be uniform for all the antigens to be assessed, an accurate quantitative analysis is restricted to one fluorescent molecule per antigen at a time. In addition to FRET, other possible physical phenomena that can affect the fluorescence quantitation include self-absorption and quenching; these processes are also distance dependent. Future research pertaining to the characterization or design of QDs for multiplex quantitation and for minimizing fluorescence cross-talk will be needed.

One clear advantage of QD-based staining and subsequent measurement of target antigens on tissues is the improved accuracy in quantification as compared to methods currently used in laboratory settings. Pathology scoring, the most widely used method of quantitative immunohistochemistry in clinical settings, assigns a numerical scoring system of 0 to 4 for quantification of tumor antigens, with aggressive lesions being given a higher number demonstrating a higher grade. The assessment of antigen expression using this method is on a discontinuous scale (i.e., nominal values of 0, 1, 2, 3, or 4). Moreover, the human eye is not capable of discerning subtle differences of the antigen expression level. This is particularly the case in a high and low end of the expression scale. In contrast to pathology-based scoring, the QD-based method described here provides protein expression measurement of antigens in a continuous scale. This in turn makes the detection of even small changes in tumor progression possible and may lead to a more accurate and sensitive tumor classification. The use of fluorescence molecules through acquisition of high-power images for protein quantification is another method for assessment of protein level. However, organic dyes are highly susceptible to photobleaching. The loss of fluorescent signal in traditional dyes is well established[11,30] and could affect the accuracy of protein quantification. We tested the stability of a QD signal as compared to Alexa 488, one of the most stable fluorescent dyes,[31] using our FFPE A549 lung carcinoma xenograft

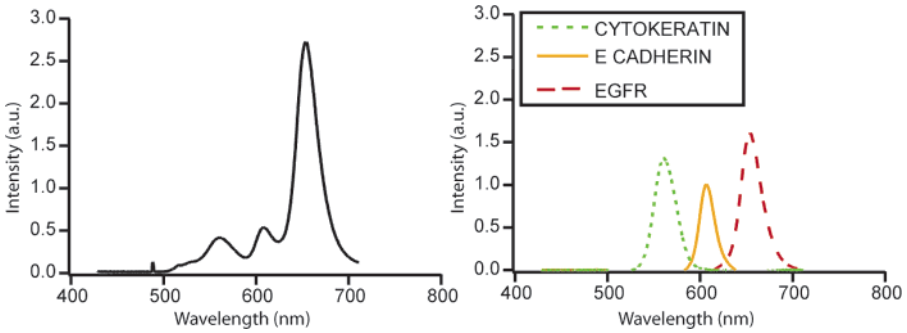

Figure 5. Effect of FRET on quantification of multiplexed protein markers. QD immunolabeling of EGFR, E-cadherin, and cytokeratin on a FFPE A549 lung carcinoma tissue section in a multiplex staining experiment (left) and in separate staining experiments (right). The spectra in the multiplexed staining experiment show different values than the expected level of protein expression for EGFR, E-cadherin, and cytokeratin obtained from individual staining. The 655 nm signal from EGFR is greatly enhanced, whereas the 605 and 565 nm signals obtained from E-cadherin and cytokeratin, respectively, are reduced in fluorescence intensity.

platform. The signal obtained from QD immunostaining for EGFR showed no reduction in signal intensity during continuous irradiation of a UV laser for 30 min, whereas the fluorescent signal from Alexa 488 showed 70% reduction in signal intensity during the same exposure time (Supporting Information). In addressing these two problems, the QD signal could provide a more accurate means of measurement of signal intensity and quantification of tumor-derived antigens in cancer biopsies.

In conclusion we have shown the quantitative analysis of tissue microarray using the QD-based immunoprofiling of proteins discussed here enabled accurate measurements of tumor-derived antigen and delineated expression profiles of archival cancer tissue specimen. The use of QD in conjunction with optical spectroscopy provided a tool to obtain a sensitive, accurate and quantitative measurement on a continuous scale not attainable by traditional methods. The dedicated algorithms developed herein provided an automated mathematical tool to remove autofluorescence, normalize tumor protein expression to cellular content, and produce a comprehensive profile of tumor derived antigen on a tissue microarray. The use of our method and algorithms can be expanded to encompass the study of a myriad of protein markers. This comprehensive analysis provides the means to study diagnostic or prognostic factors or perhaps a group of markers involved synergistically in carcinogenesis. Taken together, QDs offer a novel strategy and quantitative measure for examination of clinical specimens and pathology-based diagnosis of cancer.

Acknowledgment. The authors acknowledge James Ho for his technical expertise in immunostaining, Ming Li for his help in xenograft tumors, and Suzanne Lau for RT-Q-PCR. The authors thank Dr. Travis Jennings for helpful discussions on FRET. This work has been funded through CIHR (W.C.W.C., B.C.W., and M.S.T.) and NSERC, CFI, and OIT (W.C.W.C.). Furthermore, this project was partially funded by Genome Canada through Ontario Genome Institute.

Supporting Information Available: A detailed description of the experimental procedures, fluorescent imaging controls, and photostability study. This material is available free of charge via the Internet at http://pubs.acs.org.

References

(1) Kononen, J.; Bubendorf, L.; Kallioniemi, A.; Barlund, M.; Schraml, P.; Leighton, S.; Torhorst, J.; Mihatsch, M. J.; Sauter, G.; Kallioniemi, O. P. *Nat. Med.* **1998**, *7*, 844−847.
(2) Uhlen, M.; Ponten, F. *Mol. Cell. Proteomics* **2005**, *4*, 384−393.
(3) Dolled-Filhart, M. P.; Rimm, D. L.; Stroobant, P. *Pers. Med.* **2005**, *4*, 291−300.
(4) Pedersen, L.; Holck, S.; Schiodt, T.; Zedeler, K.; Mouridsen, H. T. *Breast Cancer Res. Treat.* **1989**, *1*, 91−99.
(5) Cregger, M.; Berger, A. J.; Rimm, D. L. *Arch. Pathol. Lab. Med.* **2006**, *7*, 1026−1030.
(6) Henriksen, K. L.; Rasmussen, B. B.; Lykkesfeldt, A. E.; Moller, S.; Ejlertsen, B.; Mouridsen, H. T. *J. Clin. Pathol.* **2006**.
(7) van Gijssel, H. E.; Schild, L. J.; Watt, D. L.; Roth, M. J.; Wang, G. Q.; Dawsey, S. M.; Albert, P. S.; Qiao, Y. L.; Taylor, P. R.; Dong, Z. W.; Poirier, M. C. *Mutat. Res.* **2004**, *1*−2, 55−62.
(8) Robinson, J. P. *Methods Cell Biol.* **2001**, 89−106.
(9) Rao, J.; Seligson, D.; Hemstreet, G. P. *BioTechniques* **2002**, *4*, 924−6, 928−30, 932.
(10) Camp, R. L.; Chung, G. G.; Rimm, D. L. *Nat. Med.* **2002**, *11*, 1323−1327.
(11) Bernas, T.; Robinson, J. P.; Asem, E. K.; Rajwa, B. *J. Biomed. Opt.* **2005**, *6*, 064015-1.
(12) Baschong, W.; Suetterlin, R.; Laeng, R. H. *J. Histochem. Cytochem.* **2001**, *12*, 1565−1572.
(13) Niki, H.; Hosokawa, S.; Nagaike, K.; Tagawa, T. *J. Immunol. Methods* **2004**, *1*−*2*, 143−151.
(14) DaCosta, R.; Wilson, B.; Marcon, N. *Dig. Endoscopy* **2003**, 153−73.
(15) Yeh, H. C.; Ho, Y. P.; Wang, T. H. *Nanomedicine* **2005**, *2*, 115−121.
(16) Klostranec, J.; Chan, W. C. W. *Adv. Mater.* **2006**, *18*, 1963.
(17) Mews, A.; Kadavanich, A. V.; Banin, U.; Alivisatos, A. P. *Phys. L Rev. B*: *Condens. Matter Mater. Phys.* **1996**, *20*, R13242−R13245.
(18) Santra, S.; Dutta, D.; Walter, G. A.; Moudgil, B. M. *Technol. Cancer Res. Treat.* **2005**, *6*, 593−602.
(19) Gao, X.; Cui, Y.; Levenson, R. M.; Chung, L. W.; Nie, S. *Nat. Biotechnol.* **2004**, *8*, 969−976.
(20) Chan, W. C.; Nie, S. *Science* **1998**, *5385*, 2016−2018.
(21) Cai, W.; Shin, D. W.; Chen, K.; Gheysens, O.; Cao, Q.; Wang, S. X.; Gambhir, S. S.; Chen, X. *Nano Lett.* **2006**, *4*, 669−676.
(22) Le Gac, S.; Vermes, I.; Van den Berg, A. *Nano Lett.* **2006**, *6*, 1863−1869.
(23) Eastman, P. S.; Ruan, W.; Doctolero, M.; Nuttall, R.; de Feo, G.; Park, J. S.; Chu, J. S.; Cooke, P.; Gray, J. W.; Li, S.; Chen, F. F. *Nano Lett.* **2006**, *5*, 1059−1064.
(24) Zhang, T.; Stilwell, J. L.; Gerion, D.; Ding, L.; Elboudwarej, O.; Cooke, P. A.; Gray, J. W.; Alivisatos, A. P.; Chen, F. F. *Nano Lett.* **2006**, *4*, 800−808.
(25) DaCosta, R. S.; Wilson, B. C.; Marcon, N. E. *Curr. Opin. Gastroenterol.* **2005**, *1*, 70−79.

(26) Kidd, M.; Modlin, I. M.; Mane, S. M.; Camp, R. L.; Eick, G.; Latich, I. *Ann. Surg. Oncol.* **2006**, *2*, 253−262.
(27) Förster, T. *Ann. Phys* **1948**, 55.
(28) Chen, Y.; Mills, J. D.; Periasamy, A. *Differentiation* **2003**, *9*−*10*, 528−541.
(29) Periasamy, A. *J. Biomed. Opt.* **2001**, *3*, 287−291.
(30) Alivisatos, A. P.; Gu, W.; Larabell, C. *Annu. Rev. Biomed. Eng.* **2005**, 55−76.
(31) Panchuk-Voloshina, N.; Haugland, R. P.; Bishop-Stewart, J.; Bhalgat, M. K.; Millard, P. J.; Mao, F.; Leung, W. Y.; Haugland, R. P. *J. Histochem. Cytochem.* **1999**, *9*, 1179−1188.

NL062111N